
Automating High Quality RT Planning at Scale

Riqiang Gao^{1*} Mamadou Diallo¹ Han Liu¹ Anthony Magliari² Jonathan Sackett²
Wilko Verbakel² Sandra Meyers³ Masoud Zarepisheh⁴ Rafe Mcbeth⁵
Simon Arberet¹ Martin Kraus¹ Florin C. Ghesu¹ Ali Kamen¹

¹Digital Technology and Innovation, Siemens Healthineers

²Varian Medical Systems, Siemens Healthineers

³University of California San Diego

⁴Memorial Sloan Kettering Cancer Center

⁵University of Pennsylvania

Abstract

Radiotherapy (RT) planning is complex, subjective, and time-intensive. Advances in artificial intelligence (AI) promise to improve its precision, efficiency, and consistency, but progress is often limited by the scarcity of large, standardized datasets. To address this, we introduce the Automated Iterative RT Planning (AIRTP) system, a scalable solution for generating high-quality treatment plans. This scalable solution is designed to generate substantial volumes of consistently high-quality treatment plans, overcoming a key obstacle in the advancement of AI-driven RT planning. Our AIRTP pipeline adheres to clinical guidelines and automates essential steps, including organ-at-risk (OAR) contouring, helper structure creation, beam setup, optimization, and plan quality improvement, using AI integrated with RT planning software like Varian’s Eclipse. Furthermore, a novel approach for determining optimization parameters to reproduce 3D dose distributions, i.e. a method to convert dose predictions to deliverable treatment plans constrained by machine limitations. A comparative analysis of plan quality reveals that our automated pipeline produces treatment plans of quality comparable to those generated manually, which traditionally require several hours of labor per plan. Committed to public research, the first data release of our AIRTP pipeline includes nine cohorts covering head-and-neck and lung cancer sites to support an AAPM 2025 challenge. This data set features **more than 10 times** the number of plans compared to the largest existing well-curated public data set to our best knowledge.

Repo: github.com/RiqiangGao/GDP-HMM_AAPMChallenge.

1 Introduction

Radiation therapy (RT) is a critical treatment modality used in approximately 50% of all cancer cases. Deep learning approaches have been incorporated into various stages of the RT planning process, including dose prediction [17, 6, 12], fluence prediction [22], leaf sequencing [11], and dose calculation [23]. Among recent advancements in RT, 3D dose prediction emerges as a particularly promising innovation. This approach directly estimates 3D dose distributions from inputs such as CT scans, PTV/OAR masks, and planning configurations, eliminating the need for labor-intensive optimization processes. Dose prediction serves multiple purposes, including supporting optimization

*Corresponding author: riqiang.gao@siemens-healthineers.com.

objectives [6, 5], enabling quality assurance [13, 14], and functioning as a key component in fully AI-driven planning pipelines [11].

RT planning is a complex and subjective process involving multiple domain experts, making data curation from existing clinical plans highly labor-intensive due to human variability in contouring PTVs/OARs and planning practices. For instance, the number of OARs contoured and the quality of plans can vary significantly (see more in Sec. 2.1). Variations in radiotherapy planning introduce biases into training data, which are further exacerbated when data is collected from multiple cohorts. Additionally, most dose prediction studies face challenges such as a limited number of training patients and difficulties in quantitatively assessing quality metrics. Within the same institution, plan quality can also fluctuate over time due to the adoption of upgraded optimization technologies or updates to treatment protocols. These changes lead to inconsistencies in plan quality, further complicating the data used for AI training and evaluation.

AI-based organ segmentation has achieved significant advancements in both research and commercial applications. Varian Medical Systems’ Eclipse, a widely used platform for optimizing radiotherapy treatment plans for cancer patients, supports automation through its Eclipse Scripting API (ESAPI). ESAPI enables developers to access and manipulate patient data for planning purposes, streamlining traditionally manual tasks performed via the Eclipse Graphics User Interface (GUI). This functionality enhances workflow efficiency and ensures greater consistency in radiotherapy planning.

In this work, we present an automatic iterative radiotherapy planning (AIRTP) pipeline designed for both major radiotherapy plan modes²: Intensity-Modulated Radiation Therapy (IMRT) and Volumetric Modulated Arc Therapy (VMAT). The AIRTP pipeline replicates the human RT planning process by combining AI-based segmentation with Eclipse scripting. Our key contributions can be summarized as follows:

- Our AIRTP pipeline significantly reduces planning time from the typical 3–6 hours manually to just 0.3–1 hour automatically, enabling large-scale AI training with high-quality plans.
- We introduce an iterative refinement strategy that improves plan quality without requiring human intervention.
- We develop a method to replicate 3D dose distributions in both complex IMRT and VMAT scenarios using AIRTP, facilitating the evaluation of dose prediction impacts on deliverable dose planning.
- We have released the largest cleaned planning dataset to date for an AAPM challenge³ and beyond. This dataset: 1) contains over 10 times more plans than the existing curated public dataset [6], and 2) offers more practical settings to support diverse research explorations.

2 Method

2.1 Challenges of Clinical Plans for AI Training

The variability in radiation therapy (RT) planning data poses significant challenges for training AI models. This variability stems from differences in PTV/OAR contouring styles, planning preferences, auxiliary structures, clinical protocols, and human biases.

Variations in contouring methods—such as differences in margins, anatomical boundaries, or slice intervals—introduce noise and bias, hindering the ability of models to generalize across different clinics or clinicians. Additionally, non-standardized planning preferences, including dose constraints and optimization strategies, lead to diverse and sometimes conflicting data inputs. As shown in Fig. 1, the number of clinically contoured OARs per patient varies significantly, complicating the normalization of plan quality to a consistent standard.

²A simplified introduction to radiotherapy and its terminologies is provided in Appendix A of [11].

³The GDP-HMM is one of the selected challenges by the AAPM Working Group on Grand Challenges in 2025 (www.aapm.org/GrandChallenge).

Table 1: The heterogeneity of RT structure naming. There are thousands of unique names for PTVs and OARs across cohorts due to varied convention, making data curation difficult for AI training.

Cohort	# Patients	ROI	# Unique Names	Name Examples
In-house cohort	702	PTV	336	PTV5000, ptv inside, 3PTV_5600, 2PTV w ON, PTVplanning, PTV 70, 2PTV_4800Uniform, 2PTV_P, ptv-temp, lptv w, lptv inf, PTV46 Original, lleft PTV
		OAR	2597	Brain1, Brain.partial, BrainStem.PRV, Cord High + .5, Cord, LarynxGSL, Left BP, OC, OC uninvolved, OC wo, OC-lips, OC.Lips, ON.03, OralCavity, OralCavity.JJC, OralCavity with 5445 PTV, COLD PTV6996, FINAL PTV69, MIN PTV66,
TCIA (5 cohorts)	690	PTV	1539	Opti.PTV60, PTV 60 OPTI.AP.0.AP, PTV 60 old, PTV 66 Sup, PTV EXP, PTV HD, PTV NECK, PTV
		OAR	3694	PAROTIDES Brain DNU, Brain Push, Brachial Plexus, Brain sub, Brain2, Brainstem expd, Bstem.PRV, Cord + 0.5cm, Cord< 45, Cord.PRV, Cord+3, Cord+5mm

This lack of uniformity complicates the development of robust, generalized AI models that can learn effectively and be applied across multiple institutions. Additionally, much of the available RT data—whether from public sources (e.g., TCIA cohorts) or in-house clinical datasets—lacks clear, optimization objective definitions, making it difficult to align planned structures with the resulting RT dose maps. Table 1 highlights the heterogeneity in RT structure naming, which results in noisy matches between inputs and outputs, further complicating model training. Additionally, some clinical plans were created more than five or ten years ago, when radiotherapy technology was less advanced. As a result, these plans may not meet the higher quality standards enabled by current technology. This highlights the need for re-planning RT treatments using the latest advancements while preserving the original clinical intent.

Related Work. A closely related effort is the OpenKBP challenge [6]. Table 2 outlines the key differences between our approach and the OpenKBP data curation pipeline. Our work advances AI-based dose prediction by enhancing treatment planning across several dimensions. Specifically, we address more practical and diverse scenarios, including a broader range of treatment sites, variable prescribed doses tailored to individual patients, and an expanded set of ROI structures. Our dataset is also substantially larger, containing over ten times the number of plans compared to OpenKBP. Additionally, our plans are generated using one of the latest and most advanced planning systems—Eclipse 18.0.1 (released in 2023 by Varian Medical Systems). Unlike OpenKBP, our methodology aligns with current clinical guidelines for both planning objectives and quality assessment, ensuring greater relevance to real-world clinical practice.

Knowledge-based planning (KBP) is closely related to our AIRTP pipeline. Both traditional KBP methods (e.g., RapidPlanTM [20]) and deep-learning methods (e.g., [6, 12]) leverage previous knowledge to inform current planning, automating conventional planning processes to some extent. However, these techniques have not yet been utilized for large-scale, deliverable planning. For example, RapidPlan is integrated into the Eclipse system, but it is primarily used to estimate optimization objectives, and the overall planning process still requires significant manual effort. In contrast, our study incorporates a high-quality RapidPlan model [18] as part of AIRTP, automating the entire planning process and enhancing the quality of RapidPlan through iterative refinement.

2.2 Automatic High Quality Planning at Scale

The auto-planning pipeline consists of several steps, including auto-contouring, rule-based structure operations in order to create optimization helper structures, Eclipse engine as the main optimizer,

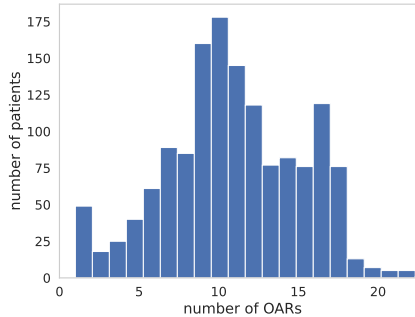


Figure 1: Number of clinically contoured OARs varies significantly across patients.

Table 2: The comparison of our auto-planning and OpenKBP pipeline. The # patients and # plans are the numbers used in GDP-HMM challenge, the total number for our internal research topics is more.

Attribute	OpenKBP [6]	Ours	Comments
Treatment Site	HaN	HaN & Lung	
Prescribed doses	Fixed	Variable	OpenKBP change original clinical intent (PTV contours and prescription) to make data homogeneous. We keep the original clinical intent with the clinical prescription.
Number of PTVs	Up to 3	Up to 3	
Planning Tool	CERR [2003]	Eclipse [v.2023]	Eclipse is from a leading Radiotherapy company Varian and widely used in clinical practice.
# Plans	340	> 4000	
# Patients	340	> 1500	
Quality Assessment	No	Yes	We use the clinical Score card to evaluate the plan quality and remove or re-plan corner cases
# Structures	up to 10/site	up to 50/site	Structures in our pipeline are Table 3 and 4.

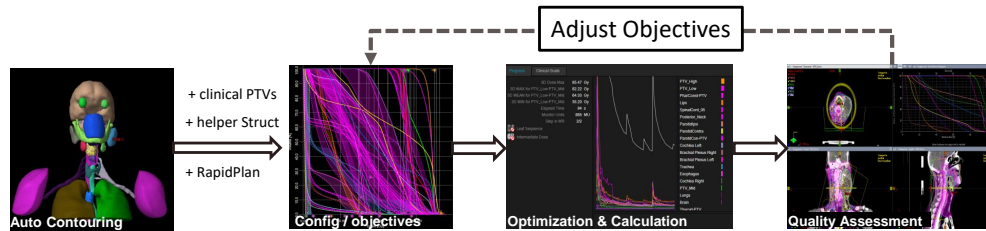


Figure 2: Illustration of automated iterative RT planning (AIRTP) pipeline. The auto contouring, helper structures are executed with C++/python code. Curated data (CT and RTSTRUCT) are stored in DICOM format, and then imported into Eclipse system. Beam configuration, RapidPlan setup, photon optimization, dose calculation, quality assessment are conducted with Eclipse Scripting API.

scripting approach to iteratively run the optimization based on RapidPlan derived objectives, and planning quality assessment, as illustrated in Fig. 2.

Step 1: RT structures creation. As shown in Fig. 3, we first contour all the needed OARs based on AI Rad Companion of Siemens Healthineers [16]. According to [18], we create PTV helpers including ring structures and OAR_i -PTV, which are necessary as part of the RapidPlan [18] optimization dose objective derivation. The structures and the associated descriptions are shown in Table 3. All the structures are saved in DICOM format and are imported together with CT series, to the Eclipse workstation.

Step 2: Planning Script. There are three major modules in the planning script. *Beam configuration* includes setting up the fractions, beam geometries, and machine parameters. For each patient, we have both IMRT and VMAT setups following the same clinical goals. For the optimizer and dose calculation, we use TrueBeam with Photon Optimization version PO.18.0.1 and Dose Calculation AXB 18.0.1, respectively. To balance the time cost, the optimization convergence is set to ‘On’ for VMAT.

For head-and-neck cancer treatment, we use four arcs for VMAT, alternating gantry rotations (CW and CCW) and setting collimator positions at 30° and 330° . For IMRT, we create two plans per patient using 9 and 15 evenly spaced angles. The objective definitions of the initial plan are primarily based on the RapidPlan model, following structure mapping. The RapidPlan model is obtained from the official Varian Medical Systems website [2].

For lung cancer treatment, we use three different angle ranges based on the tumor’s location, measured by the lateral distance from the isocenter to the patient’s mid-sagittal plane. If the distance exceeds 5 cm, we select either the left or right lung template, depending on the tumor’s side. If the distance is

Table 3: HaN RT structures for RapidPlan [18] and scorecard [2].

PTV & Helpers	Comments	PTV & Helpers	Comments
PTVHigh	PTV with the largest prescription	RingPTVHigh	$[(PTVHigh + 30mm) - (PTVHigh + 2mm)]$ AND Body
PTVHighOPT	$PTVHigh - (BrachialPlexus + 2mm)$		
PTVMid	PTV with the middle prescriptions	RingPTVMid	$[(PTVMid + 30mm) - (PTVMid + 2mm) - (PTVHigh + 6mm)]$ AND Body
PTVMidOPT	$PTVMid - (PTVHigh + 3mm)$	PTVMid-PTVHigh	as the structure name
PTVLow	PTV with the lowest prescription	RingPTVLow	$[(PTVLow + 30mm) - (PTVLow + 2mm) - (PTVMid + 6mm) - (PTVHigh + 9mm)]$ AND Body
PTVLowOPT	$PTVLow - (PTVMid + 3mm) - (PTVHigh + 6mm)$	PTVLow-PTVMid	as the structure name
PTVTotal	union of all PTVs		

OARs	OARs	OARs	OARs-PTV
BrachiaPlexus	Larynx	Posterior.Neck	Larynx-PTV
Brain	Lens_L	Shoulders	Mandible-PTV
BrainStem	Lens_R	SpinalCord	OCavity-PTV
BrainStem_03	Lips	SpinalCord_05	ParotdCon-PTV
Chiasm	OpticNerve_L	Submandibular	ParotdIps-PTV
Cochlea_L	OpticNerve_R	Trachea	Parotids-PTV
Cochlea_R	OralCavity	Lungs	PharCost-PTV
Esophagus	Parotids	Mandible	Submand-PTV
Eyes	PharynxConst	Body	SubmandL-PTV
LacrimaGlands	Pituitary	TMJoint	SubmandR-PTV

Table 4: Initial lung optimization objectives.

ROI	Type	Dose	Volume	Operation	Prior
PTV	Point	60 Gy	100 %	Lower	300
PTV	Point	63 Gy	0 %	Upper	300
BodyRing	Point	63 Gy	0 %	Upper	250
TotalLung-GTV	Point	20 Gy	18.5 %	Upper	100
TotalLung-GTV	Point	5 Gy	32.5 %	Upper	100
TotalLung-GTV	Mean	5 Gy	N/A	Upper	100
SpinalCord	Point	22 Gy	0 %	Upper	80
Heart	Point	55 Gy	0 %	Upper	60
Heart	Mean	5 Gy	N/A	Upper	60
LAD	Point	55 Gy	0 %	Upper	60
Esophagus	Mean	15 Gy	N/A	Upper	60
BrachPlexus	Mean	15 Gy	N/A	Upper	60
GreatVessels	Mean	55 Gy	0 %	Upper	60
Trachea	Mean	55 Gy	0 %	Upper	60
RingPTV	Mean	67 Gy	0 %	Upper	60

Table 5: Lung scorecard items.

ROI	Metric Type	Input
PTV	VolAtDose	60 Gy
CTV	VolAtDose	60 Gy
PTV	VolAtDose	57 Gy
PTV	VolAtDose	54 Gy
PTV	DoseAtVol	0.03 cc
PTV	DoseAtVol	99.5 %
TotalLung-GTV	VolAtDose	20 Gy
TotalLung-GTV	VolAtDose	5 Gy
TotalLung-GTV	MeanDose	N/A
SpinalCord	DoseAtVol	0.03 cc
Heart	DoseAtVol	0.03 cc
Heart	MeanDose	N/A
LAD	VolAtDose	15 Gy
Esophagus	DoseAtVol	0.03 cc
Esophagus	MeanDose	N/A
BrachPlexus	DoseAtVol	0.03 cc
GreatVessels	DoseAtVol	0.03 cc
Trachea	DoseAtVol	0.03 cc

5 cm or less, we choose angles that cover the full range. For IMRT, we use 7 fields (if lateral) or 9 angles, and for VMAT we use two arcs.

Step 3: Iterative Process. The initial plan is generated using RapidPlan [18] for head-and-neck treatment or mean/point objectives based on the scorecard [3] for lung treatment, as shown in Table 5. The iterative process is illustrated in Fig. 5(a). For each OAR, we extract DVH points from the current plan and apply a margin to set the objectives. Additionally, the metrics from the scorecard are included as objectives with some added margin. Evidence suggests that the plan quality will converge to a high score when the parameters are reasonably set. As shown in Fig. 5(b), we can reproduce a plan using only the 3D dose once the pipeline in Fig. 5(a) has converged.

Table 6: HaN scorecard items

ROI	Metric Type	Input	ROI	Metric Type	Input	ROI	Metric Type	Input
PTVHighOPT	VolAtDose	70.0 Gy	PTVHighOPT	DoseAtVol	99.5 %	PTVHighOPT	DoseAtVol	0.03 cc
PTVMid	VolAtDose	63.0 Gy	PTVMid	DoseAtVol	99.5 %	PTVMid-PTVHigh	VolAtDose	66.2 Gy
PTV56	VolAtDose	56.0 Gy	PTV56	DoseAtVol	99.5 %	PTV56-PTV63	VolAtDose	58.8 Gy
SpinalCord05	DoseAtVol	0.03 cc	SpinalCord05	VolAtDose	40.0 Gy	SpinalCord05	VolAtDose	30.0 Gy
BrainStem03	DoseAtVol	0.03 cc	Brain	DoseAtVol	0.03 cc	Brain	VolAtDose	50.0 Gy
Pituitary	MeanDose	N/A	Chiasm	DoseAtVol	0.03 cc	OpticNerveL	DoseAtVol	0.03 cc
OpticNerveR	DoseAtVol	0.03 cc	LacrimalGlands	MeanDose	N/A	CochleaR	VolAtDose	40.0 Gy
CochleaL	VolAtDose	40.0 Gy	LensR	DoseAtVol	0.03 cc	LensL	DoseAtVol	0.03 cc
EyeR	DoseAtVol	0.03 cc	EyeR	MeanDose	N/A	EyeL	DoseAtVol	0.03 cc
Mandible-PTV	VolAtDose	70.0 Gy	Mandible-PTV	VolAtDose	60.0 Gy	Mandible-PTV	VolAtDose	50.0 Gy
Esophagus	MeanDose	N/A	Esophagus	DoseAtVol	0.03 cc	OCavity-PTV	MeanDose	N/A
OCavity-PTV	DoseAtVol	0.03 cc	Larynx-PTV	MeanDose	N/A	Thyroid-PTV	MeanDose	N/A
BrachPlexusL	DoseAtVol	0.1 cc	BrachPlexusR	DoseAtVol	0.1 cc	SubmandL-PTV	MeanDose	N/A
SubmandR-PTV	MeanDose	N/A	TMJoint	DoseAtVol	0.03 cc	RingPTV70	DoseAtVol	0.03 cc
RingPTV63	DoseAtVol	0.03 cc	RingPTV56	DoseAtVol	0.03 cc	PosteriorNeck	VolAtDose	35.0 Gy
Trachea	MeanDose	N/A	Lungs	VolAtDose	20.0 Gy	Shoulders	MeanDose	N/A
Parotids-PTV	MeanDose	N/A	Submand-PTV	MeanDose	N/A			

Algorithm 1 Iterative Planning Processing

Input: Patient data with CT, PTV/OAR contours, helper structures, prescribed doses for PTVs; ScoreCard for plan evaluation; beam configurations; RapidPlan for a head-and-neck scenario.
Output: A series of plans until the ScoreCard convergence.

- 1: Initialize plan based on RapidPlan or ScorePlan items
- 2: **for** $n = 1$ to MAX iteration **do**
- 3: Initialize objective buffer D
- 4: **for** s in PTV and its Ring structures **do**
- 5: Set the upper / lower point objectives based prescribed dose
- 6: Use the same priorities as in the initial plan
- 7: **end for**
- 8: Calculate the ScoreCard for current plan
- 9: **for** s in ScoreCard OARs and Helpers **do**
- 10: Calculate the DVH Cumulative Data $f_s(\cdot)$
- 11: **for** v in volume points $\{1, 10, 20, 30, 40, 60, 80\}$ **do**
- 12: Calculate the dose $d = f_s(v)$
- 13: Calculate the margin and objective dose and priority based on 3.
- 14: Add the objective to objective buffer.
- 15: **end for**
- 16: **for** items in ScoreCard **do**
- 17: Calculate the margin and objective dose and priority based on 4.
- 18: Add the objective to objective buffer.
- 19: **end for**
- 20: **end for**
- 21: optimize with the current objective buffer.
- 22: update current plan.
- 23: **end for**

More detailed steps are outlined in Algorithm 1, along with some module implementations shown in Figures 3 and 4.

3 Planning and Results

3.1 Planning Environment

The first step in RT structure creation involves auto-contouring of OARs and the creation of helper structures, primarily based on clinical PTVs. The auto-contouring utilizes the latest version of AI-Rad Companion [16]. To accelerate this process, we developed a C++ executable that generates all the necessary structures with a harmonized naming convention and exports the results in DICOM format.

```

def Dose2Obj(s, value, volume, score):
    if '-PTV' in s.Id and value > 20:
        res = max(value * 0.95, value - 3)
        weight = 120
    elif value > 63 and '-PTV' not in s.Id:
        res = value - 1
        weight = 80
    elif value < 20 and (volume is not None and volume < 50):
        res = max(value * 0.95, value - 2)
        weight = 80
    elif value < 10:
        res = max(value * 0.95, value - 2)
        weight = 80
    else:
        res = max(value * 0.95, value - 2)
        weight = 120
    return round(res, 2), weight

```

Figure 3: Calculation of optimization objectives based on DVHs during the iterative process.

```

def scorecard2dose(x, ScorePoints):
    ScorePoints = sorted(ScorePoints, key=lambda p: p['PointX'])

    if x < ScorePoints[0]['PointX']:
        x = ScorePoints[0]['PointX']
    if x > ScorePoints[len(ScorePoints) - 1]['PointX']:
        x = ScorePoints[len(ScorePoints) - 1]['PointX']

    for i in range(len(ScorePoints) - 1):
        x1, y1 = ScorePoints[i]['PointX'], ScorePoints[i]['Score']
        x2, y2 = ScorePoints[i + 1]['PointX'], ScorePoints[i + 1]['Score']
        assert x1 <= x2
        # Check if x is within the current segment
        if x1 <= x <= x2:
            # Calculate the slope (m) and intercept (b) for the line between (x1, y1) and
            # (x2, y2)
            m = (y2 - y1) / (x2 - x1 + 1e-5)
            b = y1 - m * x1
            score = m * x + b
            dose_value = max(x * 0.85, x - 7) # add margin to dose value
            priority = 60 + min(abs(m), 7) * 20 / (1 + np.exp(score / 3))
            # calculate the optimization priority
            return dose_value, priority

```

Figure 4: Calculation of optimization objectives using scorecard items during the iterative process.

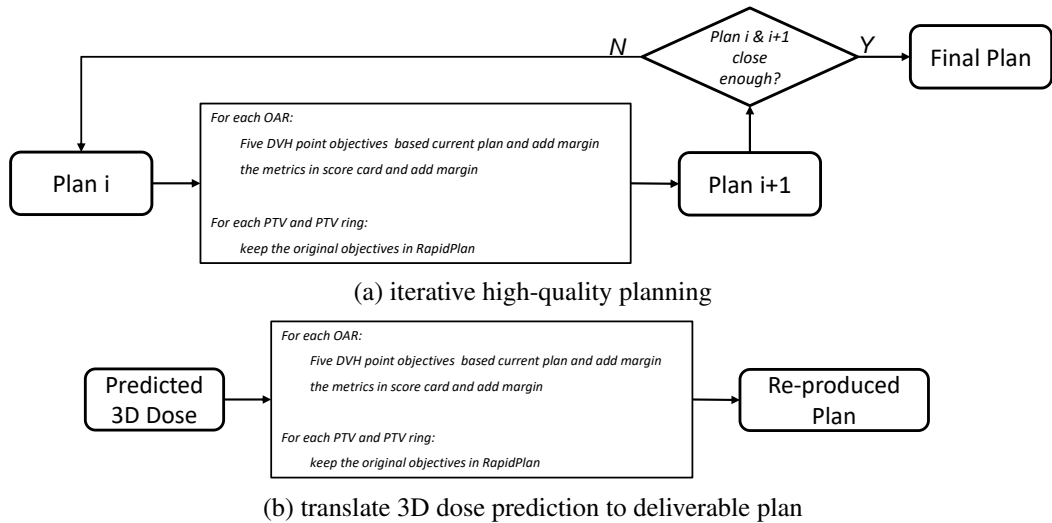


Figure 5: (a) shows the process that increase the quality of planning iteratively. (b) demonstrates the method translating predicted 3D dose to a deliverable plan. The way of defining objectives of above two pipelines are the same. The metrics in scorecard are shown in Table 6 for head-and-neck and Table 5 for lung cancer, respectively.

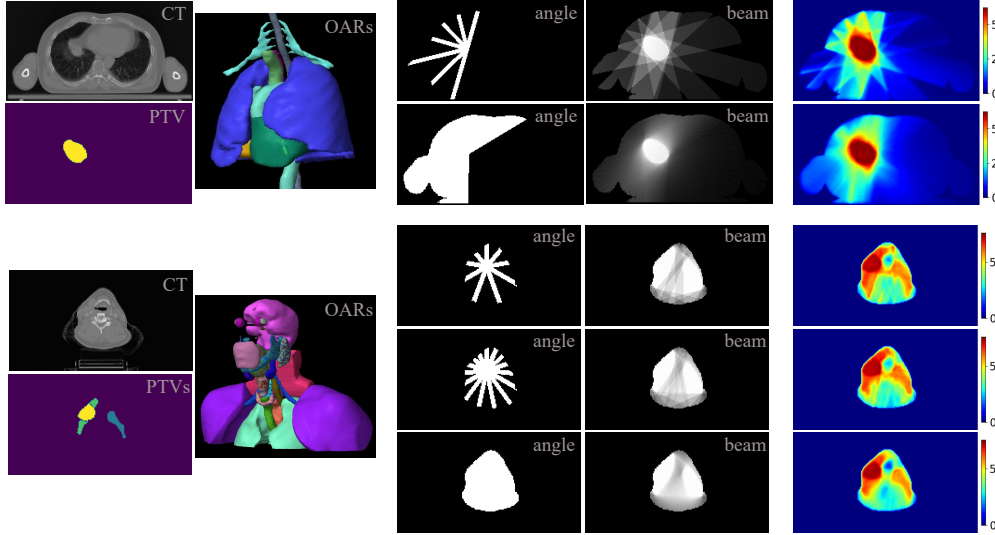


Figure 6: Examples of head-and-neck and lung plans. In the GDP-HMM challenge, each lung cancer patient has two plans: one IMRT and one VMAT; each head-and-neck cancer patient has three plans: two IMRT and one VMAT.

To run auto-planning at scale, we have built five GPU computing nodes in Microsoft Azure, in which instances of Eclipse 18.0.1 are installed. Each node has 64 GB Random-access memory (RAM) and 24 GB GPU memory. We use PyESAPI [4] and Python to import the DICOM input data and run the scripted algorithm to interact the Eclipse optimization engine. PyESAPI is a Python-based tool that enables rapid prototyping of C# based ESAPI built-in functionalities.

The public TCIA data sources (CT, PTVs, prescribed doses) that we utilized are from NSCLC-Cetuximab [9], NSCLC-Radiomics [1], Head-Neck Cetuximab [8], Head-Neck-PET-CT [19], HNC-IMRT-70-33 [10], HNSCC [15], HNSCC-3DCT-RT [7], TCGA-HNSC [24].

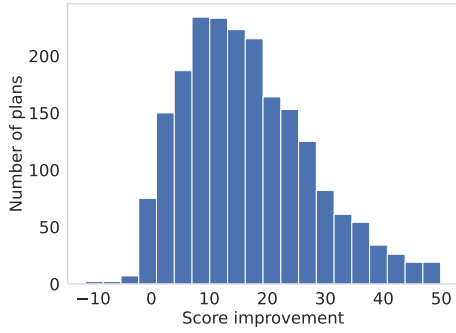
3.2 Plan Quality Analysis

Fig. 6 demonstrates plan examples for lung cancer and head-and-neck cancer patients. Our AIRTP can generate arbitrarily large number of plans with varying parameters, given sufficient time and computing resources. As the first public release of our data, we include two plans per patient for the lung site and three plans per patient for the head-and-neck site. Additional examples can be found in Appendices B and C.

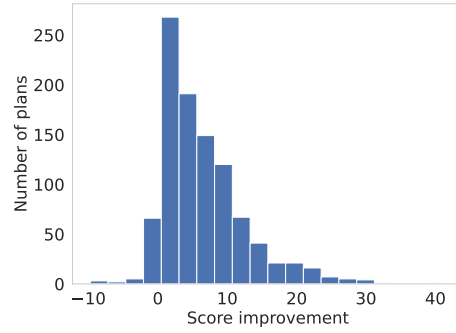
Fig. 7 demonstrates that our iterative refinement improves the plan quality of a strong RapidPlan baseline [18]. The plan quality metrics follow the a modified scorecards from [3] for lung and [2] for head-and-neck treatments, where large negative values are included when criteria are not met.

3.3 Comparison with Clinical Plans

Two randomly selected head-and-neck cases from different cohorts are illustrated in Fig. 8. One notable observation is that the AIRTP plan demonstrates improved PTV homogeneity without compromising OAR sparing. However, it is important to emphasize that we cannot definitively claim that the AIRTP plan is superior to the clinical manual plan based solely on DVHs or scorecards, as the planning process is inherently subjective and clinical plans may follow different protocols. On a positive note, we observed no significant quality drop compared to clinical plans. This fully automated AIRTP process eliminates human bias, paving the way for unbiased large-scale AI training.



(a) Score improvement of IMRT plans.



(b) Score improvement of VMAT plans.

Figure 7: Quality improvement achieved through iterative refinement across all head-and-neck cohorts.

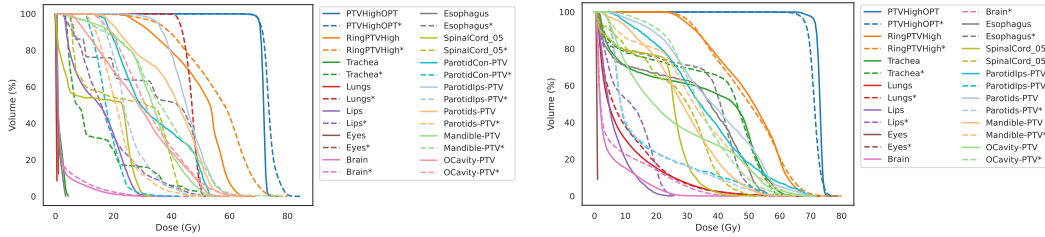


Figure 8: The DVH comparisons between our plans and clinical plans are shown, with dashed lines representing clinical plans and solid lines representing plans generated by our AIRTP pipeline.

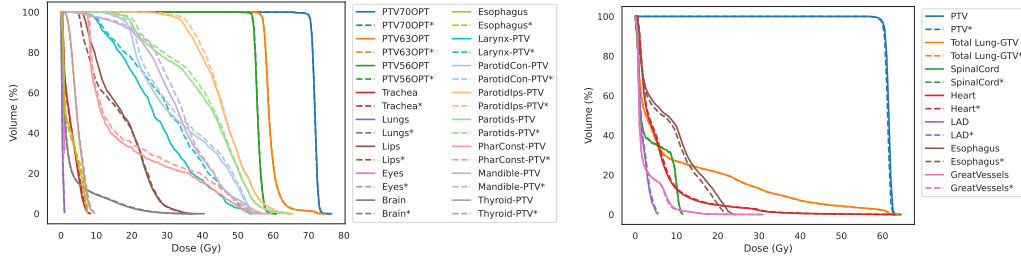
3.4 Plan Reproducibility Given 3D Dose

In Fig. 9, we illustrate both head-and-neck and lung cases regarding re-planning consistency based on 3D dose (using the method shown in Fig. 5(b)). The PTV objectives are defined according to their prescribed doses to preserve clinical intent, while the OAR objectives are extracted based on the 3D dose of the reference that needs to be reproduced, along with RT contouring.

The advantages of high plan reproducibility are twofold. First, when a dose prediction model is properly trained, it enables the rapid generation of visualized 3D dose distributions and dose-volume histograms (DVHs) based on patient data and beam configuration. This allows users to quickly assess and adjust the treatment plan. For example, a typical head-and-neck case requires approximately 20 minutes for a single forward-planning session, whereas deep learning-based dose prediction methods, such as those described in [12], can generate results in just 0.2 seconds (excluding data loading and preprocessing time). Second, this high reproducibility provides an opportunity to evaluate dose predictions in the context of downstream clinical tasks.

3.5 Beyond the Topics of GDP-HMM Challenge

Except for dose prediction, researchers have explored AI applications including fluence prediction [21], leaf sequencing [11], dose computation [23]. With our pipeline, we can create large-scale training data for all these modules. As in Fig. 10, we show a few examples of fluence maps, leaf sequences, and dose volumes generated from our pipeline.



(a) HaN: reference (solid) vs. reproduce (dash). (b) Lung: reference (solid) vs. reproduce (dash).

Figure 9: Re-planning examples following the method shown in Fig. 5(b) are provided. The closer the dashed line and solid line are to each other, the better the reproducibility of our method.

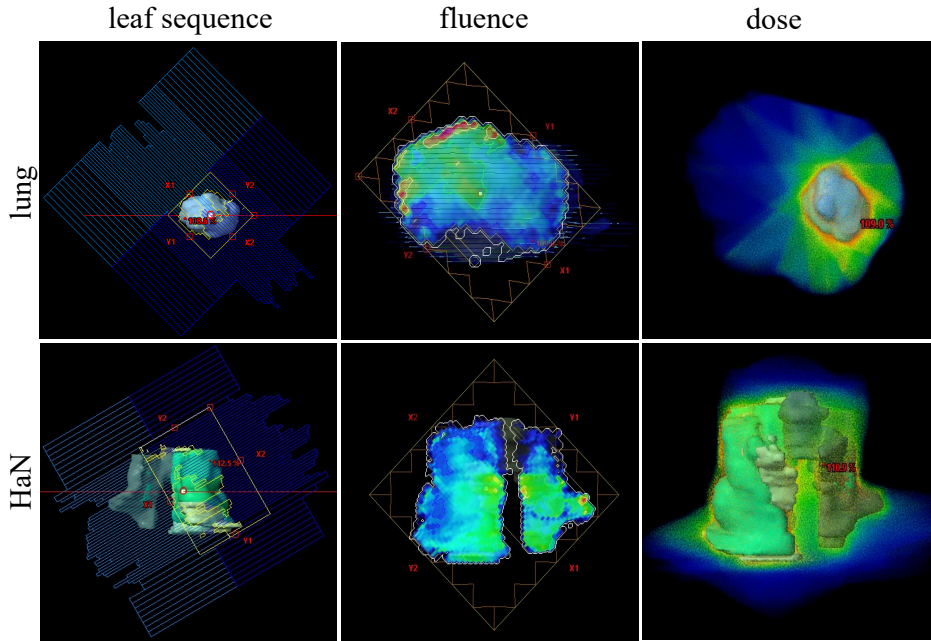


Figure 10: Data examples (screenshots from Eclipse visualization) are provided to support AI training for tasks such as leaf sequencing, fluence prediction, dose calculation, and/or their combinations.

4 Discussion

Conclusion. In this work, we propose an automated RT planning pipeline that includes OAR auto-contouring, scripted RT configuration and objective setup, scripted optimization and calculation, as well as automated iterative refinement guided by quality evaluation. The results from our pipeline have been used in the GDP-HMM challenge, one of few challenges selected by the AAPM community. Our proposed method, along with the released dataset, has the potential to advance the field of artificial intelligence in radiotherapy.

As an initial step toward automating high-quality planning at scale, our work has several limitations compared to expert planning in clinical practice. **First**, clinical planning involves detailed patient-specific considerations, such as variations in the contouring of PTVs/OARs, auxiliary structures, and various dose constraints. In our pipeline, we focus primarily on clinical PTVs and prescribed doses as the key patient-specific factors, simplifying the process due to the lack of access to more detailed patient data. **Second**, different institutions often follow different protocols, and even within the same institution, planners may have individual preferences. Our pipeline does not currently account for such subjective variations. While these preferences are partially reflected in the scorecards, we use only

one standardized scorecard per treatment site. A future direction is to collaborate with dosimetrists to develop multiple scorecards that better capture diverse clinical preferences and practices. **Third**, unlike more well-established research fields, our comparative analyses of iterative refinement and re-planning strategies are limited by the lack of directly relevant literature. Although we made efforts to compare the DVHs of AIRTP plans with clinically approved plans, this comparison may not be entirely fair, as the AIRTP and clinical plans follow different guidelines. **Fourth**, the summary and clinical impact analysis of the GDP-HMM challenge are beyond the scope of this paper and will be provided following the conclusion of the challenge.

Outlook. Compared to other AI domains such as natural language processing and computer vision, the availability of large-scale training data in medical imaging is often limited. In radiotherapy, this challenge is further amplified by the complexity, subjectivity, noise, and limited scale of clinical data, as discussed in Section 2.1. Despite these obstacles, our work represents a significant step toward enabling large-scale AI research in radiotherapy. Notably, our pipeline is designed to be flexible, making it possible to simulate data at scale with sufficient computational resources and time. We envision this pipeline as a foundational tool for advancing AI applications in radiotherapy and facilitating future research in this critical field with more required data.

Disclaimer. The information in this paper is based on research results that are not commercially available. Future commercial availability cannot be guaranteed.

References

- [1] H. Aerts, L. Wee, E. Rios Velazquez, R. Leijenaar, C. Parmar, P. Grossmann, S. Carvalho, J. Bussink, R. Monshouwer, B. Haibe-Kains, et al. Data from nslc-radiomics (version 4)[data set]. *The Cancer Imaging Archive*, 2014. 8
- [2] V. M. Affairs. Bilateral head&neck 70/63/56gy (hn-sib-bpi) [rapidplan]. <https://medicalaffairs.varian.com/hn-sib-bpi-rapidplan-vmat2>, 2024. Accessed: 2024-10-19. 4, 5, 8
- [3] V. M. Affairs. Lung - conventional 60gy (nrg lu-004 / atkins km 2021). <https://medicalaffairs.varian.com/lung-conventional-vmat2>, 2024. Accessed: 2024-10-19. 5, 8
- [4] V. M. Affairs. Python interface to eclipse scripting api. <https://github.com/VarianAPIs/PyESAPI>, 2024. Accessed: 2024-12-10. 8
- [5] A. Babier, R. Mahmood, B. Zhang, V. G. L. Alves, A. M. Barragán, B. Barragán-Montero, J. Beaudry, C. E. Cardenas, Y. Chang, Z. Chen, J. Chun, K. Diaz, H. David Eraso, E. Faustmann, S. Gaj, S. Gay, M. Gronberg, B. Guo, J. He, G. Heilemann, S. Hira, Y. Huang, F. Ji, D. Jiang, J. Carlo, J. Giraldo, H. Lee, J. Lian, S. Liu, K.-C. Liu, J. Jos´, J. Marrugo, K. Miki, K. Nakamura, T. Netherton, D. Nguyen, H. Nourzadeh, A. F. I. Osman, Z. Peng, J. Darío, Q. Muñoz, M. Muñoz, C. Ramsel, D. J. Rhee, J. David Rodriguez, H. Shan, J. V. Siebers, M. H. Soomro, K. Sun, A. A. Andrés, U. Hoyos, C. Valderrama, R. Verbeek, E. Wang, S. Willems, Q. Wu, X. Xu, S. Yang, L. Yuan, S. Zhu, L. Zimmermann, K. L. Moore, T. G. Purdie, A. L. McNiven, and T. C. Y. Chan. OpenKBP-Opt: An international and reproducible evaluation of 76 knowledge-based planning pipelines. *Physics in Medicine & Biology*, 2022. 2
- [6] A. Babier, B. Zhang, R. Mahmood, K. L. Moore, T. G. Purdie, A. L. McNiven, and T. C. Y. Chan. OpenKBP: The open-access knowledge-based planning grand challenge. *Medical Physics*, 2020. 1, 2, 3, 4
- [7] T. Bejarano, M. Ornelas-Couto, and I. Mihaylov. Head-and-neck squamous cell carcinoma patients with ct taken during pre-treatment, mid-treatment, and post-treatment (hnscc-3dct-rt)[dataset], 2018. 8
- [8] W. Bosch, W. Straube, J. Matthews, and J. Purdy. Head-neck cetuximab-the cancer imaging archive. *The Cancer Imaging Archive*, 2015. 8

- [9] J. Bradley and K. Forster. Data from nslc-cetuximab. the cancer imaging archive, 2018. 8
- [10] J. Buatti, C. Kabat, R. Li, S. Sivabaskar, M. de Oliveira, N. Papanikolaou, S. Stathakis, N. Paragios, and N. Kirby. Ct-rtstruct-rtdose-rtplan sets of head and neck cancers treated with identical prescriptions using imrt: An open dataset for deep learning in treatment planning (version 1) [data set]. the cancer imaging archive., 2024. 8
- [11] R. Gao, F.-C. Ghesu, S. Arberet, S. Basiri, E. Kuusela, M. Kraus, D. Comaniciu, and A. Kamen. Multi-agent reinforcement learning meets leaf sequencing in radiotherapy. In *International Conference on Machine Learning*, 2024. 1, 2, 9
- [12] R. Gao, B. Lou, Z. Xu, D. Comaniciu, and A. Kamen. Flexible-cm gan: Towards precise 3d dose prediction in radiotherapy. In *Proceedings of the IEEE/CVF Conference on Computer Vision and Pattern Recognition*, pages 715–725, 2023. 1, 3, 9, 16
- [13] M. P. Gronberg, B. M. Beadle, A. S. Garden, H. Skinner, S. Gay, T. Netherton, W. Cao, C. E. Cardenas, C. Chung, D. T. Fuentes, C. D. Fuller, R. M. Howell, A. Jhingran, T. Y. Lim, B. Marquez, R. Mumme, A. M. Olanrewaju, C. B. Peterson, I. Vazquez, T. J. Whitaker, Z. Wooten, M. Yang, and L. E. Court. Deep Learning–Based Dose Prediction for Automated, Individualized Quality Assurance of Head and Neck Radiation Therapy Plans. *Practical Radiation Oncology*, 2023. 2
- [14] M. P. Gronberg, A. Jhingran, T. J. Netherton, S. S. Gay, C. E. Cardenas, C. Chung, D. Fuentes, C. D. Fuller, R. M. Howell, M. Khan, T. Y. Lim, B. Marquez, A. M. Olanrewaju, C. B. Peterson, I. Vazquez, T. J. Whitaker, Z. Wooten, M. Yang, and L. E. Court. Deep learning–based dose prediction to improve the plan quality of volumetric modulated arc therapy for gynecologic cancers. *Medical Physics*, 2023. 2
- [15] A. Grossberg, H. Elhalawani, A. Mohamed, S. Mulder, B. Williams, A. L. White, J. Zafereo, A. J. Wong, J. E. Berends, S. AboHashem, et al. Hnsc. *The Cancer Imaging Archive*, 2020. 8
- [16] S. Healthineers. Ai-rad companion. <https://www.siemens-healthineers.com/en-us/digital-health-solutions/ai-rad-companion>, 2024. Accessed: 2024-09-19. 4, 6
- [17] X. Kui, F. Liu, M. Yang, H. Wang, C. Liu, D. Huang, Q. Li, L. Chen, and B. Zou. A review of dose prediction methods for tumor radiation therapy. *Meta-Radiology*, page 100057, 2024. 1
- [18] A. Magliari, R. Clark, L. Rosa, and S. Beriwal. Hn-sib-bpi: A single click, sub-site specific, dosimetric scorecard tuned rapidplan model created from a foundation model for treating head and neck with bilateral neck. *Medical Dosimetry*, 2024. 3, 4, 5, 8
- [19] M. Vallieres, E. Kay-Rivest, L. J. Perrin, X. Liem, C. Furstoss, N. Khaouam, P. F. Nguyen-Tan, C.-S. Wang, and K. Sultanem. Data from head-neck-pet-ct the cancer imaging archive, 2017. 8
- [20] Varian. Rapidplan knowledge-based planning. <https://www.varian.com/products/radiotherapy/treatment-planning/rapidplan-knowledge-based-planning>, 2024. Accessed: 2024-09-19. 3, 14
- [21] M. Wang, Q. Zhang, S. Lam, J. Cai, and R. Yang. A Review on Application of Deep Learning Algorithms in External Beam Radiotherapy Automated Treatment Planning. *Frontiers in Oncology*, 2020. 9
- [22] W. Wang, Y. Sheng, C. Wang, J. Zhang, X. Li, M. Palta, B. Czito, C. G. Willett, Q. Wu, Y. Ge, F. F. Yin, and Q. J. Wu. Fluence Map Prediction Using Deep Learning Models – Direct Plan Generation for Pancreas Stereotactic Body Radiation Therapy. *Frontiers in Artificial Intelligence*, 2020. 1
- [23] Y. Xing, D. Nguyen, W. Lu, M. Yang, and S. Jiang. A feasibility study on deep learning-based radiotherapy dose calculation. *Medical physics*, 47(2):753–758, 2020. 1, 9
- [24] M. Zuley, R. Jarosz, S. Kirk, Y. Lee, R. Colen, K. Garcia, D. Delbeke, M. Pham, P. Nagy, and G. Sevinc. The cancer genome atlas head-neck squamous cell carcinoma collection (tcga-hnsc). *Cancer Imaging Archive website*, 2016. 8

Appendix

Table of Contents

A Detailed Scorecard Examples	14
B Visualization of Creating Beam/Angle Plates	16
C Visualization of More Data Examples	17

A Detailed Scorecard Examples

Table 7: An example of 9-angle IMRT for head-and-neck cancer.

StructId	MetricType	Input	Output (Initial)	Score (Initial)	Output (AIRTP)	Score (AIRTP)
PTVHighOPT	VolumeAtDose	70.0 Gy	97.00 %	19.00	97.00 %	19.00
PTVHighOPT	DoseAtVolume	99.5 %	69.07 Gy	1.33	69.10 Gy	1.34
PTVHighOPT	DoseAtVolume	0.03 CC	74.83 Gy	8.55	74.50 Gy	8.78
PTVLow	VolumeAtDose	56.0 Gy	99.39 %	14.90	99.36 %	14.89
PTVLow	DoseAtVolume	99.5 %	55.82 Gy	1.46	55.85 Gy	1.47
PTVLow-PTVHigh	VolumeAtDose	58.8 Gy	75.89 %	0.82	60.61 %	3.88
SpinalCord.05	DoseAtVolume	0.03 CC	45.44 Gy	5.82	46.85 Gy	5.26
SpinalCord.05	VolumeAtDose	40.0 Gy	5.42 %	1.37	3.92 %	1.61
SpinalCord.05	VolumeAtDose	30.0 Gy	45.87 %	-0.44	33.38 %	1.16
BrainStem.03	DoseAtVolume	0.03 CC	49.56 Gy	3.01	45.50 Gy	3.11
Brain	DoseAtVolume	0.03 CC	57.77 Gy	1.61	54.10 Gy	1.64
Brain	VolumeAtDose	50.0 Gy	0.64 CC	3.00	0.08 CC	3.00
Pituitary	MeanDose	None	5.50 Gy	0.95	5.74 Gy	0.95
OpticNerve.L	DoseAtVolume	0.03 CC	3.55 Gy	2.94	3.68 Gy	2.93
OpticNerve.R	DoseAtVolume	0.03 CC	3.37 Gy	2.94	3.72 Gy	2.93
Cochlea.R	VolumeAtDose	40.0 Gy	0.00 %	3.00	0.00 %	3.00
Cochlea.L	VolumeAtDose	40.0 Gy	0.00 %	3.00	0.00 %	3.00
Lens.R	DoseAtVolume	0.03 CC	1.75 Gy	2.33	1.83 Gy	2.32
Lips	MeanDose	None	24.83 Gy	2.58	20.63 Gy	4.68
Mandible-PTV	VolumeAtDose	70.0 Gy	0.00 %	5.00	0.00 %	5.00
Mandible-PTV	VolumeAtDose	60.0 Gy	0.16 %	2.00	0.01 %	2.00
Mandible-PTV	VolumeAtDose	50.0 Gy	16.75 %	1.78	10.52 %	1.86
Esophagus	MeanDose	None	17.51 Gy	3.62	19.06 Gy	3.55
Esophagus	DoseAtVolume	0.03 CC	54.07 Gy	3.05	56.14 Gy	2.98
OCavity-PTV	MeanDose	None	39.58 Gy	1.67	33.19 Gy	3.63
OCavity-PTV	DoseAtVolume	0.03 CC	59.82 Gy	1.76	57.35 Gy	1.92
RingPTVHigh	DoseAtVolume	0.03 CC	72.24 Gy	2.70	71.70 Gy	3.86
RingPTVLow	DoseAtVolume	0.03 CC	63.92 Gy	-6.82	63.11 Gy	-5.74
Posterior_Neck	VolumeAtDose	35.0 Gy	52.65 %	-2.12	45.78 %	0.68
Trachea	MeanDose	None	13.16 Gy	2.11	13.66 Gy	2.09
Lungs	VolumeAtDose	20.0 Gy	13.36 CC	1.99	12.77 CC	1.99
Shoulders	MeanDose	None	4.65 Gy	0.92	4.73 Gy	0.92
Final Score	-	-	-	95.84	-	109.70

Table 7 and 8 shows the details scores and final score from the scorecard [20] to evaluate plan qualities for IMRT and VMAT, respectively. The structures (from the automatic pipeline) too small or with too much overlap with PTVs have been removed. For each table, we have included the RT structure names (i.e., `StructId`), Metric Type, the input for the Metric Type, output value, and the score of the output. We compare the output and its value of the plans from the initial (without the iterative refining) and full AIRTP, and we find that AIRTP generally improve the quality scores.

Table 8: An example of 4-arc VMAT for head-and-neck cancer.

StructId	MetricType	Input	Output (Initial)	Score (Initial)	Output (AIRTP)	Score (AIRTP)
PTVHighOPT	VolumeAtDose	70.0 Gy	97.00 %	19.00	97.00 %	19.00
PTVHighOPT	DoseAtVolume	99.5 %	69.00 Gy	1.32	69.02 Gy	1.33
PTVHighOPT	DoseAtVolume	0.03 CC	74.39 Gy	8.86	74.19 Gy	9.01
PTVLow	VolumeAtDose	56.0 Gy	97.21 %	14.53	97.79 %	14.63
PTVLow	DoseAtVolume	99.5 %	54.51 Gy	1.17	55.11 Gy	1.30
PTVLow-PTVHigh	VolumeAtDose	58.8 Gy	45.17 %	6.36	41.23 %	6.66
SpinalCord_05	DoseAtVolume	0.03 CC	41.38 Gy	6.09	38.60 Gy	6.16
SpinalCord_05	VolumeAtDose	40.0 Gy	0.49 %	1.95	0.00 %	2.00
SpinalCord_05	VolumeAtDose	30.0 Gy	33.79 %	1.12	10.67 %	1.82
BrainStem_03	DoseAtVolume	0.03 CC	45.32 Gy	3.12	44.47 Gy	3.14
Brain	DoseAtVolume	0.03 CC	52.50 Gy	1.66	53.84 Gy	1.65
Brain	VolumeAtDose	50.0 Gy	0.08 CC	3.00	0.11 CC	3.00
Pituitary	MeanDose	None	3.33 Gy	0.97	3.27 Gy	0.97
OpticNerve.L	DoseAtVolume	0.03 CC	2.57 Gy	2.95	2.52 Gy	2.96
OpticNerve.R	DoseAtVolume	0.03 CC	2.59 Gy	2.95	3.52 Gy	2.96
Cochlea.R	VolumeAtDose	40.0 Gy	0.00 %	3.00	0.00 %	3.00
Cochlea.L	VolumeAtDose	40.0 Gy	0.00 %	3.00	0.00 %	3.00
Lens.R	DoseAtVolume	0.03 CC	1.54 Gy	2.35	1.41 Gy	2.36
Lips	MeanDose	None	23.99 Gy	3.01	17.38 Gy	5.79
Mandible-PTV	VolumeAtDose	70.0 Gy	0.00 %	5.00	0.00 %	5.00
Mandible-PTV	VolumeAtDose	60.0 Gy	0.00 %	2.00	0.00 %	2.00
Mandible-PTV	VolumeAtDose	50.0 Gy	13.75 %	1.82	7.06 %	1.91
Esophagus	MeanDose	None	13.90 Gy	3.78	12.95 Gy	3.80
Esophagus	DoseAtVolume	0.03 CC	48.52 Gy	3.19	53.59 Gy	3.06
OCavity-PTV	MeanDose	None	39.55 Gy	1.68	30.11 Gy	4.47
OCavity-PTV	DoseAtVolume	0.03 CC	58.05 Gy	1.87	57.31 Gy	1.92
RingPTVHigh	DoseAtVolume	0.03 CC	70.27 Gy	4.90	70.12 Gy	4.96
RingPTVLow	DoseAtVolume	0.03 CC	58.23 Gy	1.52	57.95 Gy	2.29
Posterior.Neck	VolumeAtDose	35.0 Gy	45.95 %	0.65	37.85 %	1.94
Trachea	MeanDose	None	10.84 Gy	2.17	8.31 Gy	2.25
Lungs	VolumeAtDose	20.0 Gy	10.97 CC	1.99	9.92 CC	1.99
Shoulders	MeanDose	None	4.20 Gy	0.93	4.56 Gy	0.92
Final Score	-	-	-	117.92	-	127.23

B Visualization of Creating Beam/Angle Plates

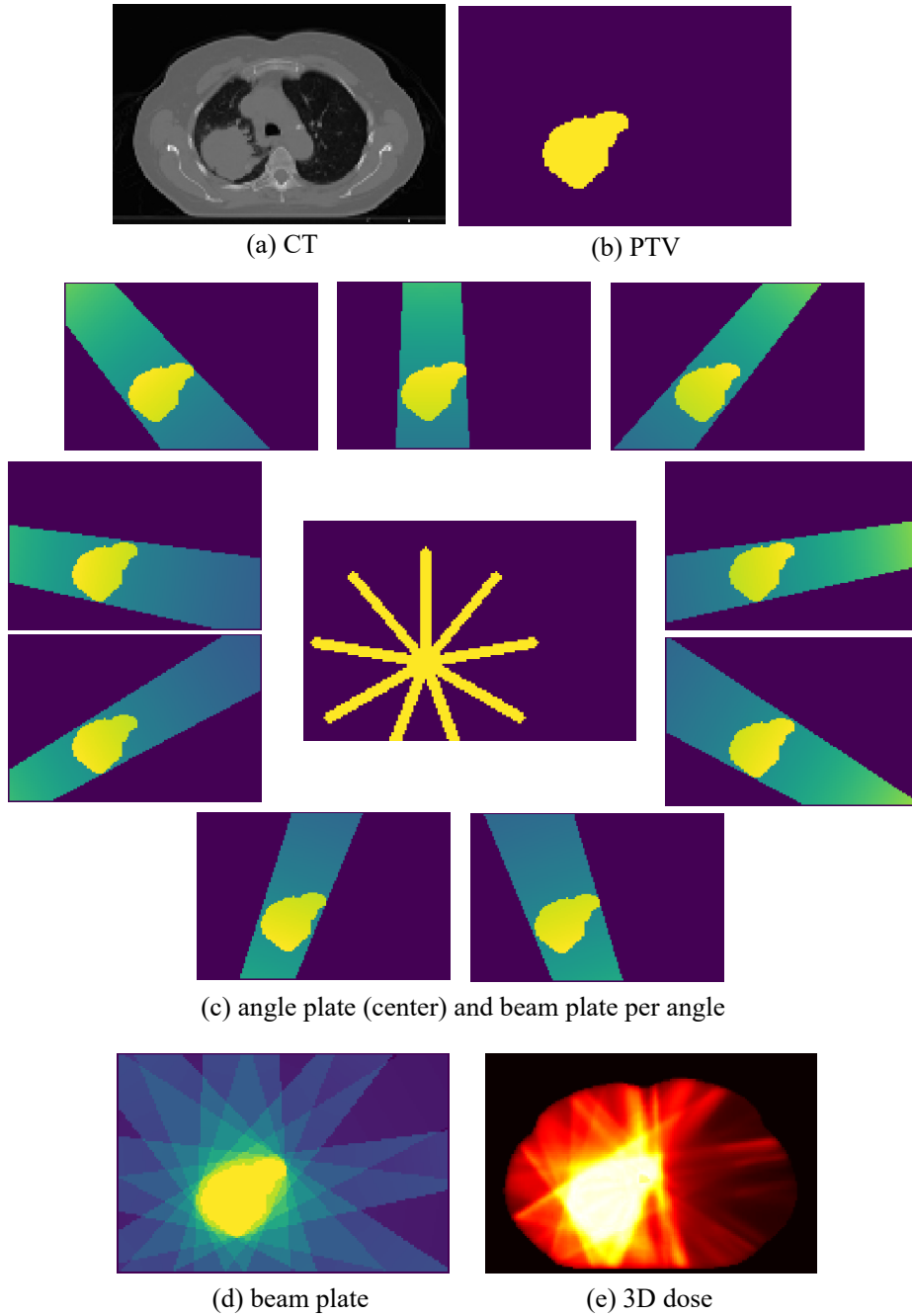


Figure 11: The example visualization of one plan with angle and beam plates. Except the angle plate, all other data are 3D though only one middle slice are used for demonstration purpose. The PTV are included in beam plate for illustrating how plates are created, but it is not necessary to be saved as part of the plate.

We include the creation of angle and beam plates in our [GDP-HMM GitHub](#), which is inspired by [12]. The angle plate gives a sketch of the angle directions, and the beam plate estimates the beam coverage considering the PTV shapes. Please follow details in the GitHub repository.

C Visualization of More Data Examples

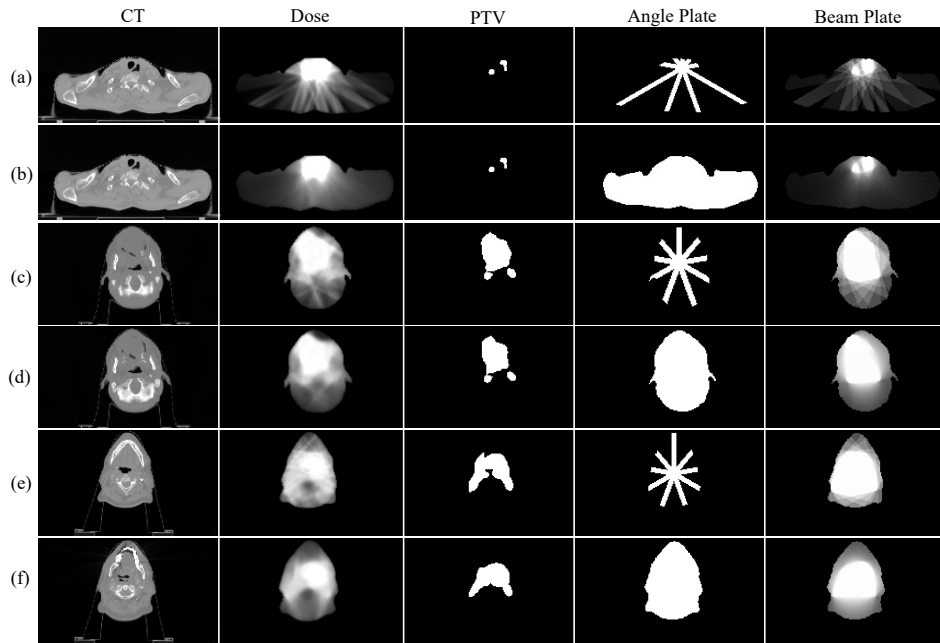


Figure 12: Six plans from three patients for head-and-neck cancer.

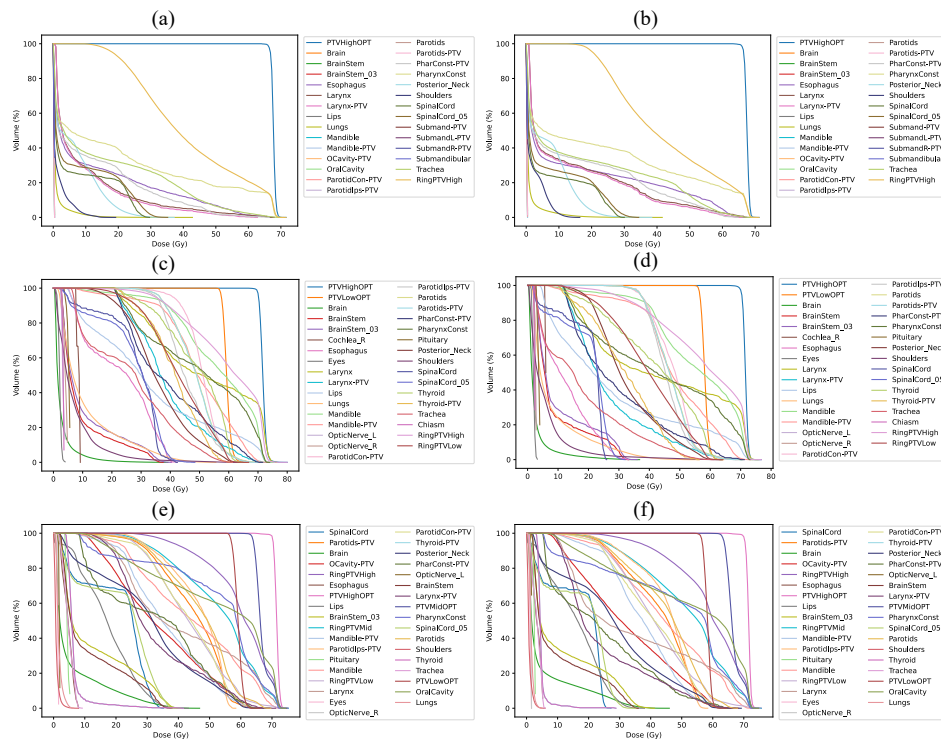


Figure 13: The DVHs of the plans shown in Fig. 12.

The creation of angle and beam plates is shown in Sec. B and documented [GDP-HMM GitHub](#). The selected three patients have one, two and three PTVs, respectively. From the DVHs, we could visually validate the quality of our plans.

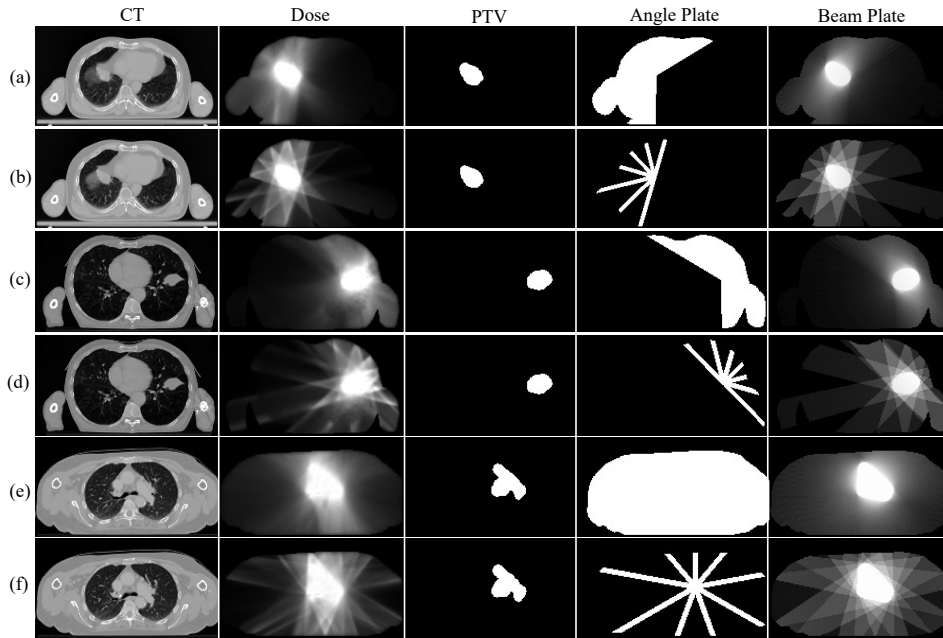


Figure 14: Six plans from three patients for lung cancer.

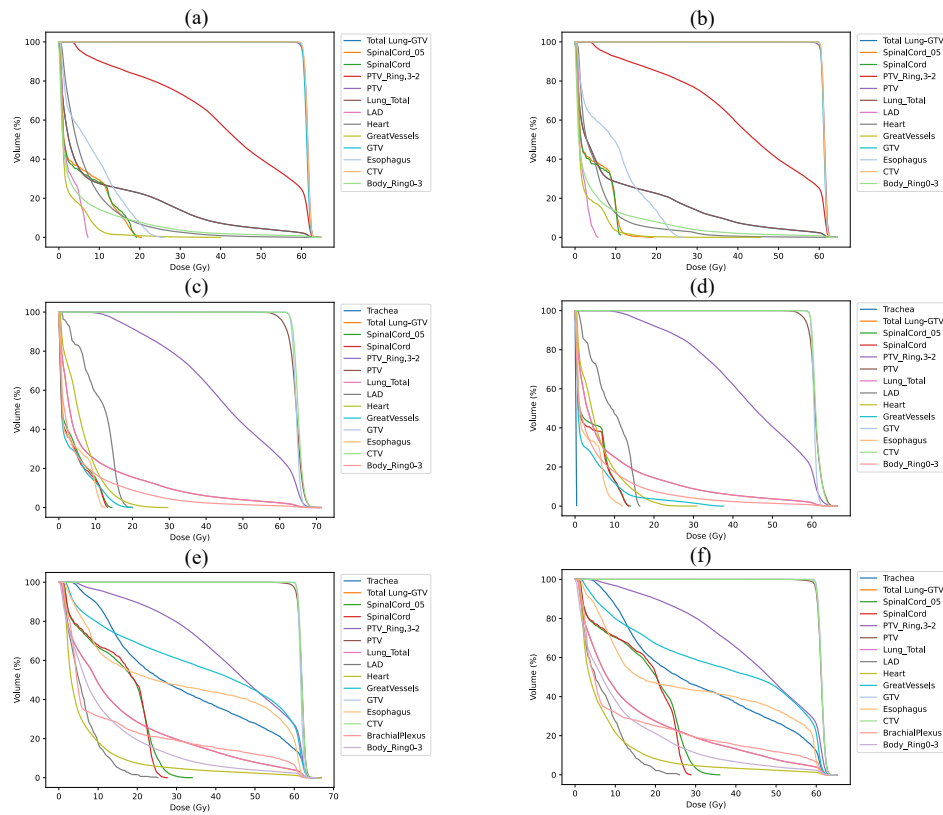


Figure 15: The DVHs of the plans shown in Fig. 14.